Journal of King Saud University – Computer and Information Sciences 33 (2021) 608–618

Contents lists available at ScienceDirect

Journal of King Saud University – Computer and Information Sciences

journal homepage: www.sciencedirect.com

Mobility assisted localization for mission critical Wireless Sensor Network applications using hybrid area exploration approach

Shamanth Nagaraju [a,*], Lucy J. Gudino [a], Nikhil Tripathi [a], Sreejith V. [a], Ramesha C.K. [b]

[a] Dept. of CS & IS, BITS Pilani, K. K. Birla Goa Campus, Goa, India
[b] Dept. of EEE, BITS Pilani, K. K. Birla Goa Campus, Goa, India

ARTICLE INFO

Article history:
Received 23 January 2018
Revised 14 April 2018
Accepted 16 April 2018
Available online 30 April 2018

Keywords:
Wireless sensor networks
Localization
Mobility model
Area exploration algorithm
Frontier
Max-gain

ABSTRACT

Sensor node location information is critical in many Wireless Sensor Network (WSN) applications with random sensor node deployment. In such applications, node localization using a faster area exploration mechanism is needed to initiate precise sensing and communication. In this paper, faster area exploration approach for mobility-assisted localization scheme is proposed for mission-critical WSN applications. Each Mobile Anchor (MA) node embedded with a localization module moves in the sensor field in a coordinated manner while localizing the deployed static nodes. The proposed area exploration scheme is implemented using a hybrid of max-gain approach and cost-utility based frontier (HMF) approach. The paper addresses the issue of sparse anchor node condition during the localization process. The simulation results obtained using Cooja simulator shows that the proposed mobility-assisted localization scheme results in accurate localization with minimum delay. The proof-of-concept of the proposed scheme is demonstrated using Berkeley static nodes and custom designed MA nodes.

1. Introduction

The Wireless Sensor Network (WSN) is composed of sensor nodes that are capable of sensing the environment, processing and communicating the sensed data to other nodes in the network. Sensor nodes strive on limited energy sources for sensing, data processing and communication. The WSN deployment is categorized as structured deployment and unstructured deployment (Lau et al., 2014). The mission-critical applications such as monitoring chemical pollution, fire and explosion, and military applications such as border area patrolling, battlefield surveillance, enemy troop monitoring and land-mine detection follows unstructured deployment where sensor nodes are randomly deployed by aerial vehicles. In such a scenario, an energy efficient localization scheme is required to detect and localize the static nodes deployed. The energy efficiency can be achieved through the mobile nodes with controlled mobility (Massaguer et al., 2006). Solving optimal mobility trajectory for mobile nodes is challenging. The mobility trajectory should be determined with the intent of improving the coverage, which can be accomplished through area exploration approaches.

The concept of area exploration started with data mules deployed to gather data from static nodes (Jea et al., 2005). Area exploration using mobile nodes finds vast applications in data gathering, network partition discovery and recovery, network diagnosis and topology mapping (Massaguer et al., 2006; Sreejith et al., 2015a). Apart from this, mobile nodes can be used to localize a set of static nodes (Amundson and Koutsoukos, 2009). It is shown in Sreejith et al. (2015a,b) that using a set of mobile nodes under controlled mobility can cover a larger area in reasonably lesser time. Due to the limited onboard power supply, the mobile nodes need to be recharged periodically for covering longer distances which can be accomplished by recharging on their own through a solar panel or inductive coupling (Phamduy et al., 2016). An energy efficient area exploration algorithm requires mobile nodes to reach each and every sensor node in minimum time and to conserve energy of both the mobile and static nodes, making it well suited for mission-critical applications. Hence, in this paper, an energy efficient area exploration approach for mobility-assisted localization scheme is proposed for the mission-critical applications.

* Corresponding author at: Dept. of CS & IS, BITS Pilani, K.K. Birla Goa Campus, Zuarinagar 403726, Goa, India.
E-mail addresses: shamanth.nagaraj@gmail.com, p20110405@goa.bits-pilani.ac.in (S. Nagaraju).
Peer review under responsibility of King Saud University.

Production and hosting by Elsevier

https://doi.org/10.1016/j.jksuci.2018.04.008
1319-1578/

The rest of the paper is organized as follows. Section 2 summarizes the background. A hybrid of max-gain and cost-utility based frontier (HMF) area exploration approach is proposed in Section 3. A distributed localization mechanism along with counteractive measures to curb the sparse anchor node condition is also explained in this section. Section 4 presents simulation results and test-bed implementation and conclusion drawn in Section 5.

2. Background

Numerous localization techniques have been proposed for WSNs in recent times. These localization techniques can be classified based on distance measurement technique, computation nature and mobility state of the nodes.

2.1. Localization based on distance measurement

The localization schemes based on distance measurement technique can be classified into two categories: range-free and range-based (Han et al., 2016). Range-free mechanisms are approximation based where network connectivity plays a pivotal role in estimating the sensor nodes' distance. The main advantage of this scheme is that it does not require any specialized hardware for localization. However, range-free localization schemes suffer from lower localization accuracy. In order to improve the localization accuracy, large number of anchor nodes are needed. The example of mobility based range-free localization schemes are Monte Carlo, Convex and Geometric Constraint approaches (Han et al., 2016).

Range-based mechanisms are more accurate compared to range-free techniques and require specialized hardware to estimate nodes' distance with reference to anchor node. Range-based localization mechanisms include Time of Arrival (ToA), Time Difference of Arrival (TDoA), Angle of Arrival (AoA) and RSSI (Received Signal Strength Indicator) (Han et al., 2016). The ToA and TDoA require strict time synchronization between the anchor and static nodes for enhancing localization accuracy. This results in higher energy consumption due to periodic time synchronization probe exchange (He et al., 2005). AoA is computationally intensive as it performs complex computations such as signal processing and measurement of the angle of signal arrival at the receiver side. Localization using RSSI suffers from lower accuracy and RSSI measurements are susceptible to environmental factors such as temperature and humidity. Mechanisms such as Kalman filter are used to eliminate the uncertainity of RSSI and thus minimize localization error (Pathirana et al., 2005).

2.2. Localization based on computation

Localization scheme based on computation is classified as centralized approach and distributed approach (Halder and Ghosal, 2016). In the centralized approach, the mobile nodes collect information such as RSSI with respect to a particular node and transmit this information to the base station for further processing. The base station then computes the position of each of these nodes and transmits the same to respective nodes. The localization with centralized approach was first proposed in Sichitiu and Ramadurai (2004). In this approach, static nodes are localized with the help of single mobile beacon node by making use of RSSI readings. Localization of nodes using single beacon node in larger areas such as battlefields is not feasible as it results in lower accuracy of localization, higher consumption of energy and time. Larger the number of mobile nodes used, better the localization accuracy and reliability. The RSSI based centralized localization scheme using multiple Unmanned Aerial Vehicle (UAV) is proposed in Perumal et al. (2014). In this scheme, all the complex localization computations are handled by a centralized server at the base station. Though this scheme claims lower computational overhead, it results in higher communication overhead as large number of packets are exchanged between UAV, static nodes and the centralized server. Increased communication overhead results in higher energy consumption as sensor node consumes more energy in radio communication compared to sensing and data processing (Pottie and Kaiser, 2000). In the distributed approach, nodes can localize themselves based on the beacon information received from several mobile nodes. Using a distributed approach for localization scheme will reduce the energy requirement and communication overhead, also it is scalable (Chelouah et al., 2017). Due to the above-mentioned advantages, RSSI based distributed localization scheme is used in the proposed localization scheme. Path-loss model and convenient calibration techniques are also used to reduce the localization estimation errors.

2.3. Localization based on mobility model

Depending on the mobility state of the anchor and sensor nodes, the localization based on mobility models are classified into four categories which are as shown in Fig. 1 (Koutsonikolas et al., 2007). The localization model proposed in this paper employs the third category, where the mobile anchor nodes are used to localize the static sensor nodes. This category of localization model is further divided into two types: random mobility and path planning. In the random mobility models such as random-walk, random-direction and random-waypoint, the mobile nodes follow the random trajectory (Camp et al., 2002), whereas, in the path planning model, the mobile nodes determine their path depending on localization conditions (Han et al., 2016). The random mobility models suffer from the sparse anchor node condition (Yong et al., 2013). The path planning based localization model overcomes the sparse anchor node condition to a certain extent. This is due to fact that the mobile nodes plan their path in such a way that each unknown node is guaranteed with at-least three anchor positions to trilaterate the nodes' location. The path planning model is further classified into static path planning and dynamic path planning (Rezazadeh et al., 2015) as shown in Fig. 1.

2.3.1. Static path planning model

In static path planning model, the Mobile Anchor (MA) node follows a predefined trajectory during the localization process. The first static path planning mobility models proposed are SCAN, DOUBLE-SCAN and HILBERT (Koutsonikolas et al., 2007). SCAN is the simplistic model, where MA nodes move in a straight line along the x or y axis. However, SCAN suffers from collinearity problem, where static nodes fail to receive beacon packets from at least three noncollinear positions to trilaterate its location. DOUBLE-SCAN and HILBERT models were proposed to overcome the collinearity problem. In DOUBLE-SCAN, the MA node is required to traverse double the distance compared to SCAN. HILBERT model is proposed in order to solve the issues of collinearity problem and larger path length. HILBERT is designed to have more curves and avoid collinearity. Though HILBERT achieved higher localization accuracy compared to SCAN and DOUBLE-SCAN, it suffered from sparse anchor node condition as it neglected the unknown nodes that are lying on the border of the area. This results in a lower localization ratio and higher localization error. To overcome collinearity problem and to improve localization accuracy, several schemes have been proposed in the literature. In localization algorithm with MA node based on Trilateration (LMAT) (Han et al., 2013) model, MA node moves according to the equilateral triangle trajectory. In Z-Curves mobile path model (Rezazadeh et al., 2014), the trajectory is built to have Z-shaped curves whereas in H-Curves model (Alomari et al., 2017) multiple sloping H-Shaped paths are

used. The LMAT, Z-Curves and H-Curves models resulted in higher localization accuracy and shorter path length.

However, the static path planning schemes described above are designed for small-scale WSN deployment and lack an efficient path planning for large-scale WSN deployment (Han et al., 2016). Once the MA node is deployed, its trajectory cannot be modified (Han et al., 2016). The exception to this is SLMAT model (Han et al., 2017), which allows the change in the trajectory of MA node on obstacle detection.

2.3.2. Dynamic path planning model

Static path planning models require terrain information beforehand to determine the path trajectory. These models are not suitable for mission-critical applications since it is difficult to obtain such an information. Dynamic path planning scheme is handy in such scenarios as it determines the path dynamically based on the demands and density of the unknown nodes. In dynamic path planning scheme, paths determined for MA nodes are deterministic and are not predefined. In Li et al. (2008), a breadth-first (BRF) algorithm and a backtracking greedy (BTG) algorithm is proposed where paths are transformed into spanning trees and MA nodes are supposed to traverse these paths dynamically based on the distribution of the unknown nodes. A mobile assisted localization by stitching (MALS) scheme is proposed for non-uniform and irregular deployment scenarios (Wang et al., 2011). In MALS scheme, the deployed network is partitioned into several units where each unit performs localization. The trajectory of MA node is formed by collating localization information of all the localization units. A deterministic dynamic beacon mobility scheduling (DREAMS) scheme is proposed in Li et al. (2012). In this scheme, initially, each MA node visits a sensor node by random movement and then performs depth-first traversal (DFT) for the deployed network. Each visited sensor node recommends the MA node to visit the unvisited neighbor. The deterministic trajectory of MA node is determined based on the relative distance between the MA and sensor node. To shorten the path length, DFT operates on local minimum spanning tree (LMST) sub-graph, whose edges are weighed by received signal strength. The unvisited but already localized sensor node may be excluded from DFT, provided its exclusion does not affect the localization of unknown sensors. The advantages of dynamic path planning models are that these schemes have shorter path length and better localization ratio, making it well suited for mission-critical applications. The drawbacks of dynamic path planning model include higher computational complexity and energy consumption since the path is determined dynamically based on the real-time information exchanged between MA and sensor nodes.

In dynamic path planning localization schemes, the area coverage is limited to the region where the node density is more. The area exploration approach for mobility-assisted localization schemes aim to provide full-area coverage. The area exploration approaches are divided into random and frontier-based (Sharma and Tiwari, 2016). In random area exploration approach, the mobile nodes follow random trajectory models such as random-walk, random-direction and random-waypoint to explore the given area. In frontier-based approaches, frontier represents the regional boundary between the explored and unexplored area, and regions are formed by combining adjacent explored cells. The frontier-based approaches converge faster compared to random mobility based approaches due to its deterministic nature (Sreejith et al., 2015a). The Near-Frontier Exploration (NFE) (Yamauchi, 1997) is a well-known frontier-based area exploration approach, where the mobile nodes choose the nearest frontier for exploration. The main drawback of NFE is that multiple mobile nodes which are deployed for area exploration may end up visiting the same area multiple times due to the lack of coordination. This problem is addressed in the Cost-Utility based Frontier (CUF) approach (Burgard et al., 2005). In CUF, utility value is assigned to each frontier cell. The utility value of each frontier cell depends on spatial information gain and the distance of frontier cell with respect to the mobile nodes. The utility value of a frontier cell is reduced when MA node visits a frontier cell. The max-gain approach (Sreejith et al., 2015b) employs an improvised strategy. In this approach, the utility function which determines mobile node trajectory considers the maximal spatial information gain and the density of mobile nodes near the cell to be explored. Unlike in frontier-based approaches, where only the cells present in the frontier are considered for exploration, the max-gain approach considers every undiscovered cell in a given map as a potential destination for the mobile node to explore. A hybrid of random-direction and cost-utility based frontier (HRF) approach is proposed in Sreejith et al. (2015a). In this approach, the random-direction mobility approach is initially followed up to certain area coverage threshold and then switches to CUF approach for faster area coverage.

The above-mentioned area exploration approaches for mobility-assisted localization schemes are energy efficient. In these localization schemes, only the mobile nodes transmit beacon packets to localize the sensor nodes. Unlike the dynamic path planning based localization schemes, there is no need for the sensor nodes to communicate with mobile nodes, thus saving a significant amount of energy for sensor nodes in an energy-scarce WSN application.

The main contributions of this paper are summarized as below.

- For area exploration, HMF (Hybrid of Max gain and cost-utility based Frontier) approach is proposed which combines max-gain approach (Sreejith et al., 2015b) and CUF approach (Burgard et al., 2005), in order to avail the advantage of both the approaches. The proposed approach initially follows the max-gain approach and then switches to the CUF approach.
- A distributed localization scheme is proposed for localizing the static nodes.
- A recursive localization algorithm is also proposed to address the localization of the nodes dealing with the sparse anchor node condition.

3. Proposed approach

The proposed approach is divided into three phases. Phase I deals with the area exploration approach for faster area coverage. Static node localization is done in phase II with the aid of MA nodes. The static nodes which are not fully localized in Phase II are localized in phase III.

3.1. Phase I: Hybrid area exploration approach

Finding the trajectory of the MA nodes for a faster area exploration is a challenging task. The CUF approach converges faster at the frontiers (Burgard et al., 2005), whereas the max-gain approach explores at a faster rate in the unexplored area (Sreejith et al., 2015b). But when multiple frontiers are created during exploration, then the performance of max-gain approach lags when compared to CUF approach. Hence, to benefit from the advantages of these two approaches, a hybrid approach is proposed which makes use of the max-gain approach at the initial phase and later switches to CUF approach for exploring the frontier region. Table 1 gives the description of the parameters used in the proposed hybrid area exploration algorithm which is explained in Algorithm 1.

Algorithm 1 Area exploration algorithm

procedure HYBRID_EXPLORATION(M, t_p, R, a, CR_k)
  $T \leftarrow R/a$
  $CV \leftarrow 0$
  for all $a_{i,j}$ **do**
    if $V(a_{i,j}) =$ BLACK **then**
      Store coordinates of $a_{i,j}$ in D_u
    end if
  end for
  while $CV < t_p$ **do**
    $CV \leftarrow NC_D/T$
    for all M_k **do** ▷ Calculating a destination cell DC_k
      for all $a_{i,j}$ **do**
        if $V(a_{i,j}) =$ BLACK **then**
          $UC_b \leftarrow count\ of\ BLACK\ cells\ in\ P(CM_k, a_{i,j})$
          $U_t(a_{i,j}) \leftarrow \alpha.\ UC_b - \sum_{k=1}^{S'_{M_k}} U_d$
          $\kappa_{i,j} \leftarrow U_t(a_{i,j}) - \beta.\ dist\ (CM_k, a_{i,j})$
          $DC_k \leftarrow max\ (\kappa_{i,j})\ , \forall a_{i,j}$
        end if
      end for
      $Mark\ P(CM_k, DC_k)\ as\ GREY\ in\ M$
      $Set\ destination\ of\ M_k\ to\ DC_k$
    end for
  end while
  while $NC_D <$ T **do**
    for all M_k **do** ▷ Calculating a destination cell DC_k among best frontier
      for all $a_{i,j}$ in the frontiers **do**
        if $V(a_{i,j}) =$ BLACK **then**
          $U_t(a_{i,j}) \leftarrow \delta - \sum_{k=1}^{S'_{M_k}} U_d$
          $\kappa_{i,j} \leftarrow U_t(a_{i,j}) - \beta.\ dist\ (CM_k, a_{i,j})$
          $DC_k \leftarrow max\ (\kappa_{i,j})\ , \forall a_{i,j}$
        end if
      end for
      $Set\ destination\ of\ M_k\ to\ DC_k$
    end for
  end while
end procedure

The static sensor nodes are deployed in a sensor field represented by polygon region S_R whose boundaries are known beforehand. For simplicity, a rectangular region R is assumed, where polygon region S_R can fit in. The region R is divided into cells a_{ij} where (i,j) represents the row and column position in region R. Each cell a_{ij} is assigned with a colour value $V(a_{ij})$ and utility value $U_t(a_{ij})$. The colour value $V(a_{ij})$ is assigned to a cell with either WHITE, BLACK or GREY to indicate whether the cell is explored, unexplored or lies on the path to destination respectively. The utility value $U_t(a_{ij})$ assigned to each cell helps the base station in determining the optimal destination cell position for MA nodes and also helps to avoid multiple MA nodes from exploring the same area. The base station maintains a common map $M = [a_{ij}]_{l\times b}$ and a data structure D_u. The common map M consists of the utility value $U_t(a_{ij})$ of each cell, whereas D_u consists of the coordinates of the unexplored cell. Based on this information, base

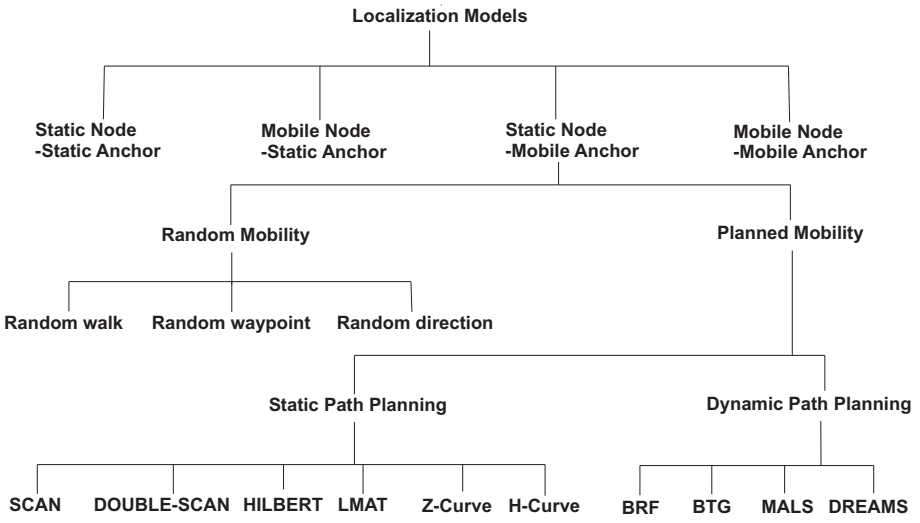

Fig. 1. Classification of mobility-assisted localization models in WSN.

Table 1
Parameters and its description for the HMF area exploration approach.

Parameters	Description
a	Unit area of a cell $a_{i,j}$.
$a_{i,j}$	Cell $a_{i,j}$ in the region R.
CM_k	Cell currently assigned to M_k.
CR_k	Communication radius of M_k.
CV	Coverage value, ratio of NC_D by T.
$dist(x,y)$	Euclidean distance between x and y.
D_u	Data structure storing coordinates of unexplored cell.
DC_k	Destination cell assigned to M_k.
$M = [a_{i,j}]_{lXb}$	Map Matrix of size $l \times b$ representing R, $\forall\ a_{i,j}$. Where l and b represents the length and breadth of the region R.
M_k	k^{th} MA node.
NC_D	Number of cells discovered (or coloured WHITE) at any point of time.
$P(j,k)$	Path coverage by MA node from j^{th} cell to k^{th} cell.
R	Rectangular region where polygon region S_R can fit in.
S_R	Sensor deployed region.
T	Total number of cells in area R.
t_p	Threshold value to run frontier approach.
U_d	Distance utility value assigned based on distance of cell $a_{i,j}$ with respect to MA node M_k.
$U_t(a_{i,j})$	Utility value of the cell $a_{i,j}$ assigned with respect to mobile node M_k.
UC_b	Number of BLACK cells lying in $P(CM_k, DC_k)$.
$V(a_{i,j})$	Colour value for cell $a_{i,j}$. WHITE indicates cell explored, BLACK indicates cell unexplored and GREY indicates the cell lying in path between MA node's current and destination position.
$\alpha,\ \beta$ and δ	Constants.
$\kappa_{i,j}$	Cost of the cell $a_{i,j}$.

station determines the destination cell for each MA node and transmits control probes to direct the MA nodes to their respective destination cell. The area exploration is performed by using several MA nodes which are initially deployed near the base station.

The coverage value CV is used to denote the area explored at any point of time t and is given by,

$$CV = \frac{NC_D}{T} \tag{1}$$

where NC_D denotes the number of cells discovered and T denotes the total number of cells in the region R which is equal to the area R divided by a. The coordinates of the unexplored cell are stored in D_u which would later be used for traversing MA nodes in these coordinate positions.

The hybrid area exploration algorithm starts initially with the max-gain approach. When the max-gain approach is followed, every point in the unexplored area is considered a possible destination for the MA node to traverse. In the proposed approach the assignment of utility value $U_t(a_{i,j})$ considers the path density of multiple MA nodes nearer to the destination cell.

In max-gain approach, base station guides each MA node to its respective destination cell DC_k. While choosing DC_k, base station considers utility value $U_t(a_{i,j})$ of all the cells. While assigning the utility value to a cell $a_{i,j}, U_d$ and UC_b are considered. Here, U_d is the distance utility value computed based on the distance between the cell $a_{i,j}$ and MA node M_k, and UC_b is the density of BLACK cells that lie on the path $P(CM_k, a_{i,j})$. U_d is calculated as,

$$U_d = \begin{cases} (1 - \frac{dist(CM_k, a_{i,j})}{CR_k}), & \text{if } dist(CM_k, a_{i,j}) < CR_k \\ 0, & \text{otherwise} \end{cases} \tag{2}$$

The utility value $U_t(a_{i,j})$ of cell $a_{i,j}$ for the max-gain approach is calculated as,

$$U_t(a_{i,j}) = \alpha.UC_b - \sum_{k=1}^{S'_{M_k}} U_d \tag{3}$$

where S'_{M_k} represents the set of MA nodes except for MA node M_k. The cost of the cell $a_{i,j}$ with respect to MA node M_k is calculated by subtracting the $dist(CM_k, a_{i,j})$ from $U_t(a_{i,j})$ which is given as,

$$\kappa_{i,j} = U_t(a_{i,j}) - \beta.\ dist\ (CM_k, a_{i,j}) \tag{4}$$

where $\kappa_{i,j}$ denotes cost of the cell $a_{i,j}$ with respect to MA node M_k and constants are denoted by α and β. Finally, DC_k denotes the destination cell allocated to M_k and is calculated as,

$$DC_k = max(\kappa_{i,j}), \forall a_{i,j} \tag{5}$$

All the cells that lie in the path $P(CM_k, DC_k)$ are marked as GREY to indicate that they are going to be explored by the MA node. It should be noted that GREY cells provide the minimum preference for other MA nodes utilizing them as destination cell or crossing those cells lying in their path. A probe will then be transmitted from base station to MA node, informing it to navigate to the destination cell DC_k. Once the MA node traverses the path $P(CM_k, DC_k)$ and reaches DC_k, all the cells in that particular path will be marked as WHITE.

Once CV exceeds threshold t_p, the CUF approach is followed. In the CUF approach, only the frontier cells are chosen as the destination point for MA nodes and the utility value $U_t(a_{i,j})$ assignment ignores the path density factor. The CUF approach continues until NC_D is equal to T. Similar to max-gain approach, the CUF approach utilises Eqs. (2)–(5) to calculate destination cell DC_k present in the closest frontier except for $U_t(a_{i,j})$ which does not consider the density of BLACK cells in $P(CM_k, DC_k)$ as given below,

$$U_t(a_{i,j}) = \delta - \sum_{k=1}^{S'_{M_k}} U_d \tag{6}$$

where δ corresponds to constant related to the CUF approach.

Once destination cell DC_k is calculated, base station directs the MA node to move to destination cell DC_k and mark the cells visited on the way as WHITE. The CUF approach continues in a loop until the entire area is explored. Once area exploration is completed, MA nodes return to the base station.

The proposed area exploration approach also takes care of obstacle detection and avoidance by MA nodes. For obstacle detection, an approach similar to Borenstein and Koren (1989) is employed to identify the obstacle's boundaries. Here, MA nodes identify the obstacle edges visible to them. The line connecting two edges is used for calculating obstacle boundaries at the base station. Based on this assumption, the base station determines the obstacle as the boundaries of the polygon and marks the respective cells falling in this obstacle region to WHITE. The cells lying in the obstacle region exert the Virtual Force Field (VFF) onto the MA nodes. The magnitude of measured VFF can be used to steer away MA nodes with the intent of avoiding the obstacles (Borenstein and Koren, 1989). To accomplish obstacle avoidance in the proposed approach, the square of the distance between the obstacle and the MA node is set to the inverse of the VFF's magnitude. The localization of static nodes is carried out simultaneously with area exploration which is explained in detail in the next section.

3.2. Phase II: Distributed localization using MA nodes

Phase II deals with the distributed localization of static nodes by MA nodes. When MA node is on move, it broadcasts beacon packets. Fig. 2 shows the beacon packet format. The target node ID field contains the broadcast address. On receiving beacon packets, RSSI values are recorded by static nodes which are further used for computing distance using log-distance path loss model described below.

The practical measurement-based propagation models indicate that the average received power decreases logarithmically with distance (Rappaport et al., 1996). Based on this notion, RSSI based ranging empirical model is used to estimate the distance (Mahapatra and Shet, 2016). According to this model,

$$P_r \propto \frac{1}{D^n} \tag{7}$$

where P_r is the received signal power, D is the distance measured in meters and n is the path loss exponent factor. Taking log on both sides and simplifying, we get,

$$10log\left(\frac{P_r}{P_{ref}}\right) \propto 10log\left(\frac{1}{D^n}\right) \tag{8}$$

The RSSI is defined as the ratio of the received power to the reference power (P_{ref}). Typically P_{ref} represents absolute value of 1mW. Hence, Eq. (8) can be written as,

$$RSSI = -10 * n * log(D) + C \tag{9}$$

where C is a constant. The above equation can be expressed as,

Target ID	Source ID	Source X Coordinate	Source Y Coordinate

Fig. 2. Beacon packet format.

$$RSSI = -m * log(D) + C \tag{10}$$

where

$$m = 10 * n \tag{11}$$

From Eq. (11), the path loss exponent factor n can be calculated as,

$$n = \frac{m}{10} \tag{12}$$

It can be observed that Eq. (10) is a linear equation with slope m and intercept C. To determine the values of m and C, a graph of measured mean RSSI values against distance in logarithmic scale is plotted. In general, plotting the results will be nonlinear which needs to be calibrated to linear scale through curve fitting model (Nagaraju et al., 2016). From Eq. (10), distance D can be derived as,

$$D = 10^{\frac{RSSI - C}{-m}} \tag{13}$$

Weighted RSSI values are used for localization purpose to address RSSI irregularities. Once the distance from the MA node to static node is calculated using Eq. (13), the coordinates of static nodes can be determined by using trilateration technique (Hong et al., 2009). Trilateration technique can be applied only when static nodes receive beacon packets from MA nodes from three different positions.

At the expiration of area exploration phase, some of the static nodes deployed in the field may not receive enough number of beacon packets to trilaterate their position. There are scenarios, where the nodes in some areas, especially at the edges will be visited only once or twice by MA nodes. In such cases, an accurate localization is impossible due to insufficient beacon packets received. Such nodes are categorized as partially localized nodes and are said to be suffering from the sparse anchor node condition (Yong et al., 2013). The solution to this problem is addressed by the mechanism proposed in phase III.

3.3. Phase III: Sparse anchor node localization

The partially localized nodes are localized by the recursive localization mechanism described in Algorithm 2.

Algorithm 2 Sparse anchor localization

Node is non-localized static node

if S_N *recieved beacon packets from MA* $\geqslant 3$ **then**
  Trilaterate location of S_N
  Set $A_N \leftarrow S_N$
  Set $p_{loc} \leftarrow 1$
else if S_N *recieved beacon packets from MA* < 3 *and Area exploration phase ends* **then**
  S_N *broadcasts* l_{req} *packets*
  Neighboring A_N *nodes responds with* l_{rep} *packets*
  Using Equation (13) calculate A_N*'s distance w.r.t* S_N
  if S_N *recieved beacon packets from MA and* A_N *put together* $\geqslant 3$ **then**
    Trilaterate location of S_N
    Set $A_N \leftarrow S_N$
    Set $p_{loc} \leftarrow 1$
  end if
end if

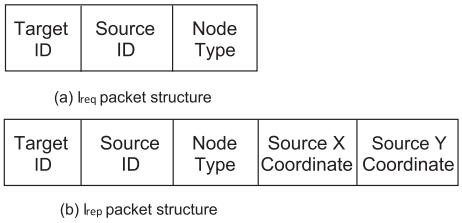

Fig. 3. Packet format of (a) l_{req} packet (b) l_{rep} packet.

Table 2
Cooja simulator configuration parameters.

Parameters	Description
Radio propagation model	Unit Disk Graph Medium (UDGM) distance loss model
MAC protocol	IEEE 802.15.4
Antenna type	Omnidirectional
Simulation area	750 m × 750 m
Data rate	250 kbps
Radio frequency	2.4 GHz
Number of MA nodes	5–9
Coverage range of antenna	50 m
Maximum transmission power	0 dBm
Receiver sensitivity	−95 dBm

Once phase II is completed, the base station needs to identify the static nodes S_N which are fully localized and partially localized by MA nodes. In order to differentiate between fully localized and partially localized S_N nodes at the beginning of phase III, flag p_{loc} is utilized. For fully localized nodes, the flag p_{loc} is set to 1 and for partially localized nodes, the p_{loc} flag is set to 0. If S_N nodes' flag p_{loc} is set to 1, it is added to the set of A_N nodes, so that it can further aid in localizing the partially localized nodes.

To localize the nodes suffering from the sparse anchor condition, special request and reply packets l_{req} and l_{rep} are used. The l_{req} packet is transmitted by partially localized nodes with the intent of getting reply l_{rep} from neighboring nodes in order to get fully localized. The l_{req} packet structure is as shown in Fig. 3(a). The target ID field contains the broadcast address so that the neighboring nodes receiving the request packet can respond with their coordinate information. Node type field of l_{req} consists of p_{loc} value which helps to differentiate partially localized nodes from other nodes. The l_{rep} packet has its first three fields similar to l_{req} packet. In addition to these fields, the next two fields consist of nodes' X and Y coordinates as shown in Fig. 3(b). If the beacon packets received from MA and A_N nodes put together is more than two, then S_N node is localized through weighted trilateration and is added to set of A_N nodes after setting its p_{loc} flag to 1.

4. Implementation and result

The simulation of the proposed HMF area exploration approach for mobility-assisted localization scheme is carried out on mobility plugin enabled Cooja simulator (Osterlind, 2014). Similar to ns-2 and ns-3 network simulators, Cooja is a discrete-event simulator. The main advantage of Cooja simulator is that it supports firmware level simulation (Jevtić et al., 2009). Also, it eases the code portability from simulation to real-time deployment (Nagaraju et al., 2017). Table 2 shows the parameters considered for the Cooja simulator to carry out the simulation of the proposed scheme.

To provide a realistic approach to simulation, the Cooja nodes are configured to emulate the WSN motes such as MicaZ by setting the nodes' maximum transmission power and receiver sensitivity to 0 dBm and −95 dBm respectively (Micaz datasheet). The simulation is carried out for nodes deployed across 750 m × 750 m with varying number of MA nodes. The transmission range of 50 m is set for both static and MA nodes. The MA nodes will periodically transmit beacon packets while traversing the trajectory, which contains MA nodes' coordinates as shown earlier in Fig. 2. Static nodes falling within the coverage range of MA nodes will store beacon information to trilaterate their location as explained in phase II and phase III of Section 3. The performance of the proposed HMF area exploration approach is compared with max-gain, HRF and CUF approaches.

Fig. 4 shows the percentage of the area discovered with reference to the simulation time for varying number of MA nodes. Based on the observations from several simulations, proposed area exploration threshold t_p is set to 75% for better results. Up to t_p is equal to 75% max-gain approach is followed. Once t_p exceeds 75%, CUF approach is followed for exploring the remaining area. It is evident from the plots that the proposed HMF approach outperforms other area exploration approaches. This is due to the fact that it avails benefits of both max-gain and CUF approaches of reaching the cells with maximal spatial information gain and faster coverage of the multiple frontiers.

Fig. 5 illustrates the path length of each area exploration approach performed with varying number of MA nodes. The path length determines the total distance traversed by the MA nodes. It can be seen from the plot that as the number of MA nodes

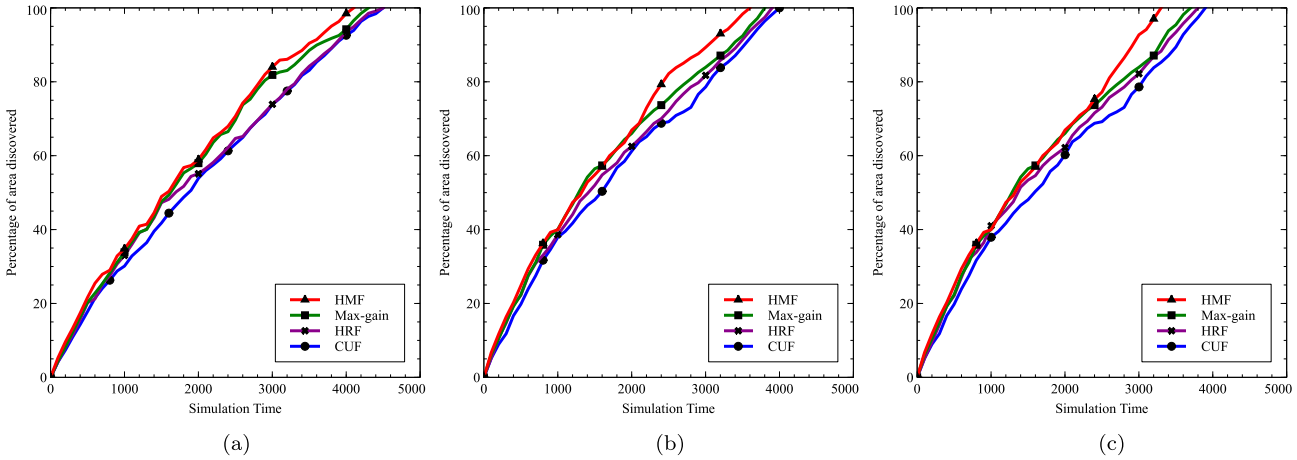

Fig. 4. Area exploration comparison for (a) 5 MA nodes, (b) 7 MA nodes and (c) 9 MA nodes.

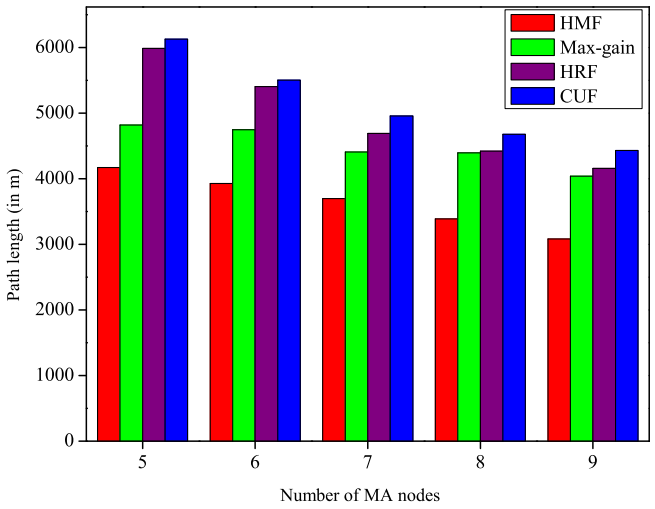

Fig. 5. Path length comparison of area exploration approaches.

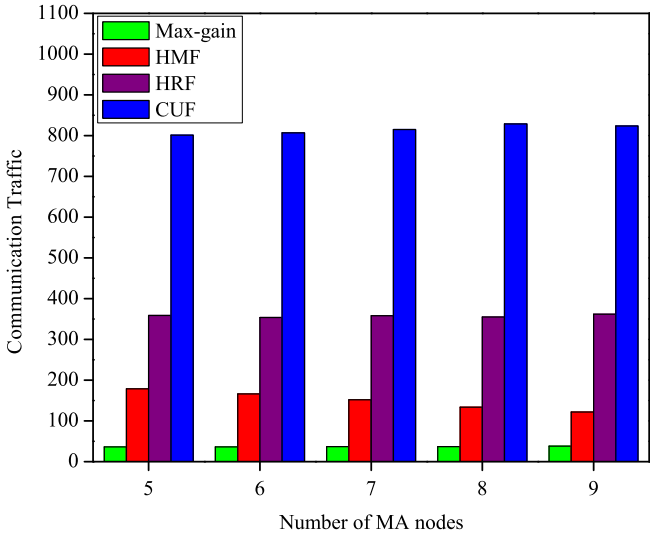

Fig. 6. Communication overhead comparison.

increases, path length decreases. The shorter path length results in lower energy consumed by MA node while traversing. HMF approach has least path length of 4170 m for 5 MA nodes and 3081 m for 9 MA nodes compared to other approaches. Hence, HMF is more energy efficient compared to other approaches. From Figs. 4 and 5, it can be deduced that shorter the path length, faster is the area coverage.

The performance of various approaches in terms of control packet communication overhead is shown in Fig. 6. Communication overhead of the proposed HMF approach is marginally higher compared to max-gain approach. Max-gain approach selects farthest destination cell for MA node thereby offering maximum spatial information gain whereas CUF approach selects nearer frontier cells. Thus, the max-gain approach accounts for minimum number of control packet exchange for communication between MA nodes and base station. Since the HMF approach is hybrid of these two approaches, it has marginally higher communication overhead when compared to the max-gain approach and performs far better than the CUF approach in terms of control packets exchanged. As the HRF approach follows random mobility in its initial phase, it has higher communication overhead when compared to the max-gain and HMF approaches. It can also be observed from Fig. 6 that

Table 3
Distance estimation error considered for assigning weights to RSSI.

Distance (in m)	RSSI (in dBm)	Distance estimation error (in m)
5	−18.68	0.27
10	−27.36	0.207
15	−35.54	0.135
20	−44.22	0.063
25	−52.4	0.003
30	−61.08	0.072
35	−69.76	0.144
40	−78.00	0.207
45	−86.62	0.279
50	−93.25	0.333

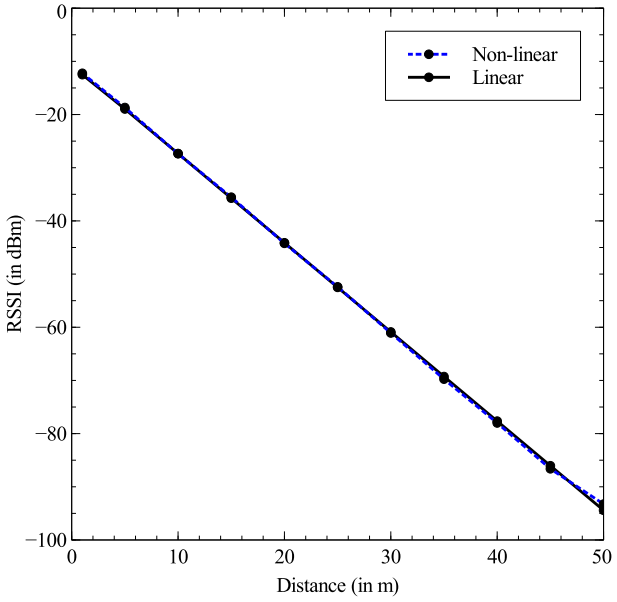

Fig. 7. Plot of the mean value of RSSI vs Distance along with calibration curve of the linear regression.

for the proposed HMF approach as the number of MA nodes increases, the number of control packets exchanged decreases.

RSSI irregularities are addressed by using weighted RSSI values. Table 3 shows the actual distance, the RSSI value obtained and corresponding distance estimation error. The distance estimation error is considered up to 50 m since the receiver sensitivity up to this range is below −95 dBm, which is the actual receiver sensitivity of CC2420 radio (Cc2420) used in MicaZ mote. The distance between the static node and MA node is estimated based on the RSSI value as specified in the Eq. (13). The distance estimation error is the difference between the actual distance and estimated distance which will be used while assigning weights. In this scheme, the RSSI value resulting in lesser distance estimation error is assigned higher weights and RSSI corresponding to higher distance estimation error is penalized by assigning lower weights. The weights that are assigned to different RSSI values are given by,

$$w_{rssi} = \frac{1}{dist_{error} + \mu} \tag{14}$$

where w_{rssi} is the weight associated with the RSSI value, $dist_{error}$ is the distance estimation error and μ is the constant relative to distance estimation error.

Based on the RSSI values shown in Table 3, the RSSI values are plotted against distance as illustrated in Fig. 7. A slightly nonlinear curve is obtained which is indicated by dotted lines. Since the intercept and slope value are required to estimate distance as per

Fig. 8. Localization of static nodes at the end of area exploration phase.

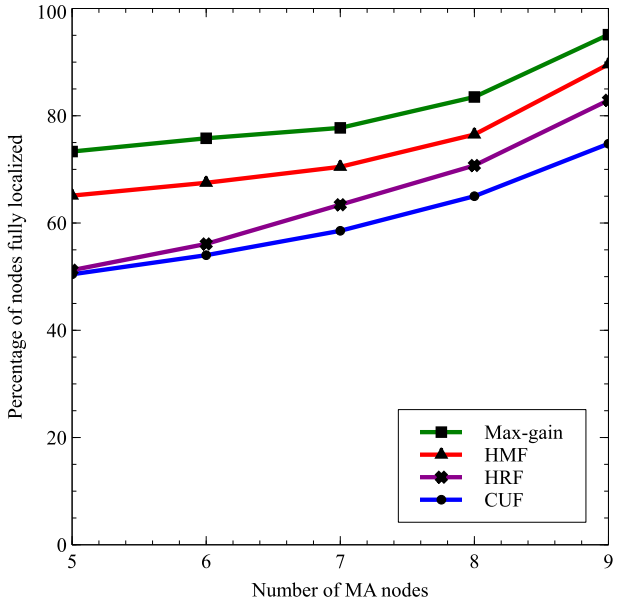

Fig. 9. Percentage of nodes fully localized at the expiration of area exploration phase.

the Eq. (13), the nonlinear curve needs to be converted to linear curve by curve fitting tool which is depicted by the solid line as shown in Fig. 7.

Fig. 8 shows the snapshot of the simulation at the expiration of area exploration phase. The simulation is carried out by 7 MA nodes, which helps in differentiating the fully localized and partially localized nodes. Here, simulation is carried out with 50 nodes, out of which nodes numbered from 1 to 7 are MA nodes and remaining are static nodes. The MA nodes are indicated by the nodes whose all three LEDs are switched OFF and the fully localized nodes have all their LEDs switched ON, whereas partially localized nodes have one or two LEDs switched ON based on the number of beacon packets received. Once area exploration phase expires, the partially localized nodes estimate their location through Algorithm 2.

Fig. 9 compares the percentage of nodes fully localized with varying number of MA nodes at the end of area exploration phase

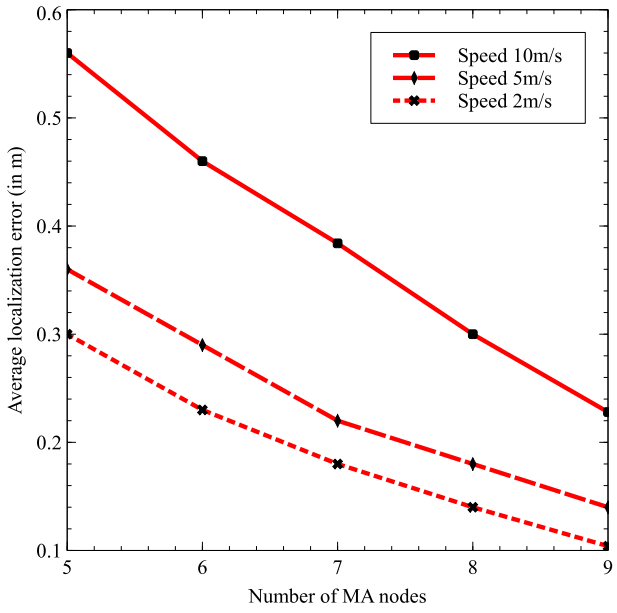

Fig. 10. Average localization error of HMF approach for MA nodes travelling at different speeds.

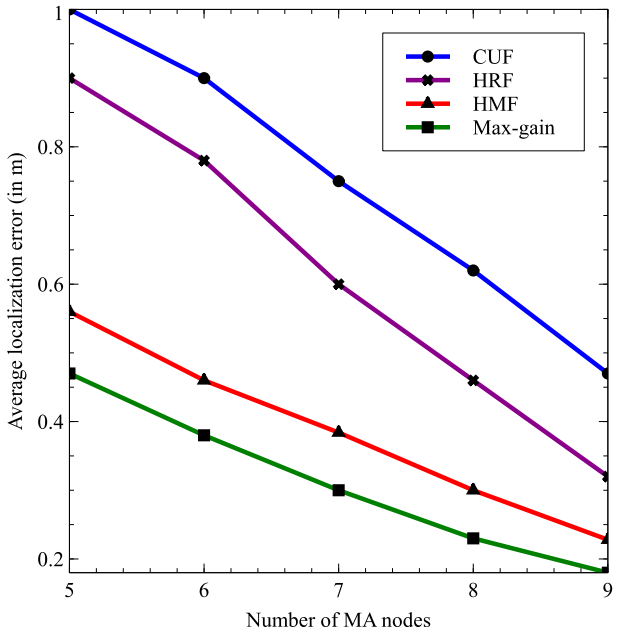

Fig. 11. Average localization error of area exploration approaches at speed of 10 m/s.

for various area exploration schemes. Max-gain approach due to its feature of covering the farthest nodes near the edges performs better than other area exploration approaches for varying number of MA nodes. The HMF approach marginally falls behind compared to the max-gain approach.

The main aim of area exploration approach for mobility-assisted localization scheme is to explore the larger area in a shorter span of time. This can be accomplished by increasing the speed of MA nodes. The next experiment is carried out to study the impact of MA nodes' speed on localization error. Fig. 10 shows the average localization error of static nodes localized by MA nodes traveling at different speeds of 10 m/s, 5 m/s and 2 m/s. These MA nodes use HMF approach for navigation due to its feature of faster

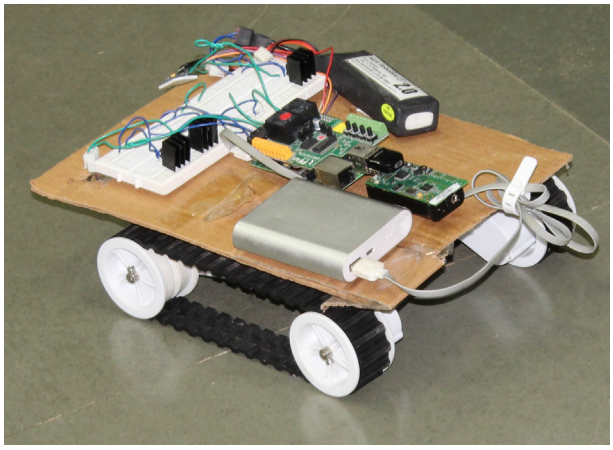

Fig. 12. Mobile robot customized for Localization.

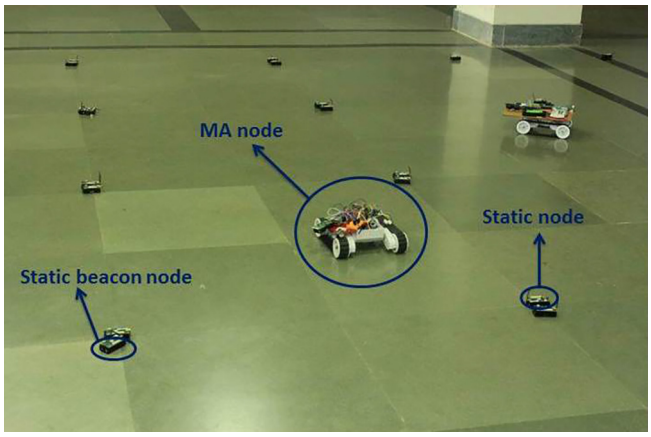

Fig. 13. Test-bed setup with 3 MA nodes, 20 MicaZ static beacon nodes and 20 MicaZ static nodes.

area coverage. As seen from the plot, when the speed of MA node increases localization error also increases. The reason behind this is some of the beacon packets may be missed out by static nodes due to the higher speed of MA nodes. It can be seen from Fig. 10 that by increasing the number of MA nodes, the average localization error decreases even when MA nodes move at higher speed.

Fig. 11 shows the average localization error of different area exploration approaches with MA node traversing at the speed of 10 m/s. It is clear from Fig. 11 that max-gain and HMF present the best results compared to the other two approaches owing to better localization ratio at the end of the area exploration phase.

Mobile robot customized for localization application is shown in Fig. 12. The mobile robot is composed of raspberrypi, a single-board processor, which is interfaced with two wireless communication modules, namely ZigBee and IEEE 802.11n for communication with the static sensor nodes and base station, respectively. Honeywell's Hmc5883l sensor is interfaced to the mobile robot for navigation assistance as it provides information about the direction of its movement.

The proof-of-concept of localization phase is done using a test-bed as shown in the Fig. 13, by deploying 3 mobile robots acting as MA nodes and 20 MicaZ static nodes, in an area of 20 m $\times$ 20 m. A grid size of 4 $\times$ 5 is used for the deployment of static nodes. MA nodes are designed using RaspberryPi for carrying out complex computations of trilateration. MA nodes communicate with the static sensor nodes by means of ZigBee radio interfaced to MA nodes. The sensor nodes' transmission range is set to $\leqslant$2 m by reducing the transceiver's power level.

Since the deployment is carried out in an indoor environment, using Global Positioning System (GPS) by MA nodes for localization is neither economical nor feasible. Also, GPS performs poorly in an indoor environment. Hence, an additional 20 MicaZ nodes acting as static beacon nodes are deployed in a grid. The grid deployment helps in pre-programming the static beacon node with the coordinates information which aids in localizing the MA nodes. Once MA nodes are localized, they further aid in localizing the static nodes. MA nodes periodically broadcast a l_{req} packet. Static beacon nodes within the MA nodes' vicinity will reply with their coordinate information through l_{rep} packet. Upon receiving l_{rep} packet, the MA nodes record the RSSI value and further trilaterates its own location. If multiple beacon packets are received by the MA node, then weights derived from the RSSI values are used to determine MA nodes' coordinates (x_u, y_u) as shown in the Eqs. (15) and (16).

$$x_u = \frac{\sum_{i=1}^{n} x_i * w_{rssi}}{n} \tag{15}$$

$$y_u = \frac{\sum_{i=1}^{n} y_i * w_{rssi}}{n} \tag{16}$$

where (x_i, y_i) is the coordinates of i^{th} beacon node, w_{rssi} is the weight associated with RSSI obtained through Eq. (14) and n is the number of beacon packets received from neighboring static beacon nodes.

For localizing static nodes, parameters such as l_{req} packet, l_{rep} packet and w_{rssi} values are used. Here, static node periodically broadcasts l_{req} packets and MA nodes which receive these packets respond with l_{rep} packet that contains its coordinates. Then again, as shown in the Eqs. (15) and (16) by using w_{rssi} values and l_{rep} packet's beacon information static node trilaterates its own location.

5. Conclusion

In this paper, a hybrid area exploration approach called HMF is proposed. The proposed HMF approach is chosen for area exploration as well as localization due to its feature of faster area coverage. The proposed approach initially follows max-gain approach till the area coverage percentage reaches threshold t_p and then switches to CUF approach. To address the localization of nodes suffering from the sparse anchor node condition, a distributed localization scheme along with a recursive localization mechanism is also proposed. The main advantage of the proposed HMF approach lies in its ability to cover a larger area in a short span of time compared to the max-gain, HRF and CUF approaches. Also, HMF approach is energy efficient since it has shorter path length for MA nodes, making it suitable for mission-critical applications. The communication overhead and localization error of the proposed HMF approach are marginally higher than that of the max-gain approach but can be reduced by increasing the number of MA nodes. For proof-of-concept, a real-time deployment with a test-bed of 3 MA nodes and 20 MicaZ static nodes are used. The comparative analysis of localization performed using area exploration and dynamic path planning models is a direction towards which future work can be enhanced.

Declarations of interest

None.

References

Alomari, A., Comeau, F., Phillips, W., Aslam, N., 2017. New path planning model for mobile anchor-assisted localization in wireless sensor networks. Wireless Netw., 1–19 https://doi.org/10.1007/s1127.

Amundson, I., Koutsoukos, X.D., A survey on localization for mobile wireless sensor networks. 2009. In: Proceedings of Second International Workshop on Mobile Entity Localization and Tracking in GPS-less Environnments, MELT2009, pp. 235–254.

Borenstein, J., Koren, Y., 1989. Real-time obstacle avoidance for fast mobile robots. IEEE Trans. Syst., Man, Cybern. 19 (5), 1179–1187. https://doi.org/10.1109/21.44033.

Burgard, W., Moors, M., Stachniss, C., Schneider, F.E., 2005. Coordinated multi-robot exploration. IEEE Trans. Rob. 21 (3), 376–386. https://doi.org/10.1109/tro.2004.839232.

Camp, T., Boleng, J., Davies, V., 2002. A survey of mobility models for ad hoc network research. Wireless Commun. Mobile Comput. 2 (5), 483–502. https://doi.org/10.1002/wcm.72.

Cc2420: 2.4 ghz ieee 802.15. 4/zigbee-ready rf transceiver, texas instruments, http://www.ti.com/lit/gpn/cc2420.

Chelouah, L., Semchedine, F., Bouallouche-Medjkoune, L., 2017. Localization protocols for mobile wireless sensor networks: a survey. Comput. Electr. Eng., 1–19 https://doi.org/10.1016/j.compeleceng.2017.03.024.

Halder, S., Ghosal, A., 2016. A survey on mobility-assisted localization techniques in wireless sensor networks. J. Netw. Comput. Appl. 60, 82–94. https://doi.org/10.1016/j.jnca.2015.11.019.

Han, G., Xu, H., Jiang, J., Shu, L., Hara, T., Nishio, S., 2013. Path planning using a mobile anchor node based on trilateration in wireless sensor networks. Wireless Commun. Mobile Comput. 13 (14), 1324–1336. https://doi.org/10.1002/wcm.1192.

Han, G., Jiang, J., Zhang, C., Duong, T.Q., Guizani, M., Karagiannidis, G.K., 2016. A survey on mobile anchor node assisted localization in wireless sensor networks. IEEE Commun. Surveys Tutorials 18 (3), 2220–2243. https://doi.org/10.1109/COMST.2016.2544751.

Han, G., Yang, X., Liu, L., Guizani, M., Zhang, W., 2017. A disaster management-oriented path planning for mobile anchor node-based localization in wireless sensor networks. IEEE Trans. Emerging Topics Comput., 1–12 https://doi.org/10.1109/TETC.2017.2687319.

He, T., Huang, C., Blum, B.M., Stankovic, J.A., Abdelzaher, T.F., 2005. Range-free localization and its impact on large scale sensor networks. ACM Trans. Embedded Comput. Syst. 4, 877–906. https://doi.org/10.1145/1113830.1113837.

Hong, S.H., Kim, B.K., Eom, D.S., 2009. Localization algorithm in wireless sensor networks with network mobility. IEEE Trans. Consum. Electron. 55 (4), 1921–1928. https://doi.org/10.1109/TCE.2009.5373751.

Jea, D., Somasundara, A., Srivastava, M., 2005. Multiple controlled mobile elements (data mules) for data collection in sensor networks, in: International conference on distributed computing in sensor systems, pp. 244–257.

Jevtić, M., Zogović, N., Dimić, G., 2009. Evaluation of wireless sensor network simulators. In: Proceedings of the 17th Telecommunications Forum (TELFOR 2009), Belgrade, Serbia, pp. 1303–1306.

Koutsonikolas, D., Das, S.M., Hu, Y.C., 2007. Path planning of mobile landmarks for localization in wireless sensor networks. Comput. Commun. 30 (13), 2577–2592. https://doi.org/10.1016/j.comcom.2007.05.048.

Lau, B.C., Ma, E.W., Chow, T.W., 2014. Probabilistic fault detector for wireless sensor network. Expert Syst. Appl. 41 (8), 3703–3711. https://doi.org/10.1016/j.eswa.2013.11.034.

Li, H., Wang, J., Li, X., Ma, H., 2008. Real-time path planning of mobile anchor node in localization for wireless sensor networks, in: Information and Automation, 2008. ICIA 2008. International Conference on, IEEE, 2008, pp. 384–389. doi: https://doi.org/10.1109/ICINFA.2008.4608030.

Li, X., Mitton, N., Simplot-Ryl, I., Simplot-Ryl, D., 2012. Dynamic beacon mobility scheduling for sensor localization. IEEE Trans. Parallel Distrib. Syst. 23 (8), 1439–1452. https://doi.org/10.1109/TPDS.2011.267.

Mahapatra, R.K., Shet, N., Experimental analysis of rssi-based distance estimation for wireless sensor networks, in: Distributed Computing, VLSI, Electrical Circuits and Robotics (DISCOVER), 2016, pp. 211–215. doi: https://doi.org/10.1109/DISCOVER.2016.7806221.

Massaguer, D., Fok, C.-L., Venkatasubramanian, N., Roman, G.-C., Lu, C., 2006. Exploring sensor networks using mobile agents. In: Proceedings of the Fifth International Joint Conference on Autonomous Agents and Multiagent Systems, pp. 323–325. doi: https://doi.org/10.1145/1160633.1160688.

Micaz datasheet, crossbow corp.,http://www.memsic.com/userfiles/files/Datasheets.

Nagaraju, S., Gudino, L.J., Kadam, B.V., Ookalkar, R., Udeshi, S., 2016. RSSI based indoor localization with interference avoidance for wireless sensor networks using anchor node with sector antennas, in: International Conference on Wireless Communications, Signal Processing and Networking (WiSPNET), pp. 2233–2237. doi: https://doi.org/10.1109/WiSPNET.2016.7566539.

Nagaraju, S., Rege, V., Gudino, L.J., Ramesha, C.K., 2017. Realistic directional antenna suite for cooja simulator, in: Twenty Third National Conference on Communications (NCC), 2017, pp. 1–6. doi: https://doi.org/10.1109/NCC.2017.8077141.

Osterlind, F., Mobility cooja plugin (2014).

Pathirana, P.N., Bulusu, N., Savkin, A.V., Jha, S., 2005. Node localization using mobile robots in delay-tolerant sensor networks. IEEE Trans. Mob. Comput. 4 (3), 285–296. https://doi.org/10.1109/tmc.2005.43.

Perumal, P., Uthariaraj, V.R., Christo, V.E., 2014. Intelligent UAV-assisted localisation to conserve battery energy in military sensor networks. Defence Sci. J. 64 (6), 557–563. https://doi.org/10.14429/dsj.64.529.

Phamduy, P., Cheong, J., Porfiri, M., 2016. An autonomous charging system for a robotic fish. IEEE/ASME Trans. Mechatron. 21 (6), 2953–2963. https://doi.org/10.1109/TMECH.2016.2582205.

Pottie, G.J., Kaiser, W.J., 2000. Wireless integrated network sensors. Communications ACM 43 (5), 51–58. https://doi.org/10.1145/332833.332838.

Rappaport, T.S., et al., 1996. Wireless communications: principles and practice, Vol. 2, Prentice Hall PTR New Jersey.

Rezazadeh, J., Moradi, M., Ismail, A.S., Dutkiewicz, E., 2014. Superior path planning mechanism for mobile beacon-assisted localization in wireless sensor networks. IEEE Sens. J. 14 (9), 3052–3064. https://doi.org/10.1109/JSEN.2014.2322958.

Rezazadeh, J., Moradi, M., Ismail, A.S., Dutkiewicz, E., 2015. Impact of static trajectories on localization in wireless sensor networks. Wireless Netw. 21 (3), 809–827. https://doi.org/10.1007/s11276-014-0821-z.

Sharma, S., Tiwari, R., 2016. A survey on multi robots area exploration techniques and algorithms, in: Computational Techniques in Information and Communication Technologies (ICCTICT), 2016 International Conference on, pp. 151–158. doi: https://doi.org/10.1109/ICCTICT.2016.7514570.

Sichitiu, M.L., Ramadurai, V., , 2004. Localization of wireless sensor networks with a mobile beacon. In: IEEE International Conference on Mobile Ad-hoc and Sensor Systems, pp. 174–183. doi: https://doi.org/10.1109/MAHSS.2004.1392104.

Sreejith, V., Anupama, K.R., Gudino, L.J., Suriyadeepan, R., 2015. Partition discovery and connectivity restoration in WSN using mobile relays. In: Proceedings of the 2015 International Conference on Distributed Computing and Networking, pp. 36:1–36:9. doi: https://doi.org/10.1145/1160633.1160688.

Sreejith, V., Anupama, K.R., Gudino, L.J., Suriyadeepan, R., 2015b. A fast exploration technique in WSN for partition recovery using mobile nodes, in. Twenty First National Conference on Communications (NCC) 2015, 1–6. https://doi.org/10.1109/NCC.2015.7084923.

Wang, H., Qi, W., Wang, K., Liu, P., Wei, L., Zhu, Y., 2011. Mobile-assisted localization by stitching in wireless sensor networks, in: Communications (ICC), 2011 IEEE International Conference on, IEEE, pp. 1–5. doi: https://doi.org/10.1109/icc.2011.5962799.

Yamauchi, B., A frontier-based approach for autonomous exploration, in: Proceedings of the IEEE International Symposium on Computational Intelligence in Robotics and Automation, CIRA'97, 1997, pp. 146–151. doi: https://doi.org/10.1109/CIRA.1997.613851.

Yong, Z., Zehui, C., Pengpeng, C., 2013. Indoor pedestrian positioning tracking algorithm with sparse anchor nodes. Int. J. Distrib. Sens. Netw. 9 (8), 1–7. https://doi.org/10.1155/2013/247306.